Proceedings of the 16th International Conference on Soil Mechanics and Geotechnical Engineering

doi:10.3233/978-1-61499-656-9-3279

Special session on the 2004 Niigata-ken Chuetsu earthquake

Séance spéciale sur le tremblement de terre de Chuetsu, Niigata, en 2004

F. Tatsuoka
Tokyo University of Science, Japan

K. Konagai
Institute of Industrial Science, University of Tokyo, Japan

T. Kokusho
Chuo University, Japan

J. Koseki
Institute of Industrial Science, University of Tokyo, Japan

M. Miyajima
Kanazawa University, Japan

1 INTRODUCTION BY TATSUOKA, F.

By the 1995 Hyogo-ken Nanbu earthquake (the 2005 Kobe earthquake), a great number of civil engineering structures and buildings were seriously damaged. Based on this experience, a very high seismic design load equivalent to the highest seismic load experienced during the Kobe earthquake (i.e., so called Level II design seismic load) was introduced into a number of seismic design codes, in particular for reinforced concrete (RC) structures, and the a-seismic design was revised accordingly. However, the revision of the a-seismic design codes for earth structures (i.e., embankments having gentle slopes, soil retaining walls, bridge abutments and others) were not revised so substantially as those for RC structures.

Nearly ten years later, by the 2004 Niigata-ken Chuetsu earthquake, a great number of infrastructures totally failed or were heavily damaged, in particular a great number of natural slopes and earth structures. It was because a strong earthquake occurred in a mountainous area and a strong rainstorm by Typhoon No. 23 hit the seismic-affected area immediately before the earthquake. The lessons from the damage and the remedial works done and to be done as well as the seismic design issues of slopes and earth structures were reported and discussed by four experts. The summary of the presentations is given below.

2 EARTHQUAKE GROUND MOTIONS AND DAMAGE TO TUNNELS BY KONAGAI, K.

2.1 *Strong motion*

An intense earthquake of magnitude 6.8 jolted Mid Niigata Prefecture, central Japan at 17:56 JST on October 23, 2004. The hypocenter of the main shock was located at 37.3 N, 138.8E with a depth of 13 km. The maximum intensity of 7 on the 7-grade Japanese intensity scale was reached.

The earthquake was followed by a series of strong aftershocks in rapid succession. The area suffered four seismic events of magnitude 6 or greater within 38 minutes after the main shock. The focal mechanisms of those major earthquakes are the reverse fault type with the compression axis oriented NW/SE, which is consistent to the historical solutions of major earthquakes in this area. Aftershocks are distributed along the northeast and southwest direction with a length of about 30km. As the time went on, aftershocks became shallower (Fig. 1). In a press release, the Geographical Survey Institute (GSI) of the Government of Japan published preliminary estimates that a fault having a length of 22 km and a width of 17 km moved approximately 1.4 m.

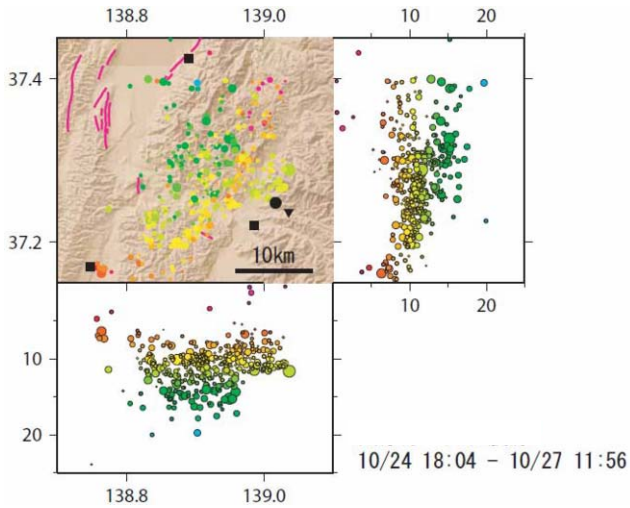

Fig. 1. Aftershocks recorded during 10/24 18:04 – 10/27 11:56 (Hirata N, 2004; source from Japan Meteorological Agency): Unusually, aftershocks scatter noticeably indicating complex fault rupturing.

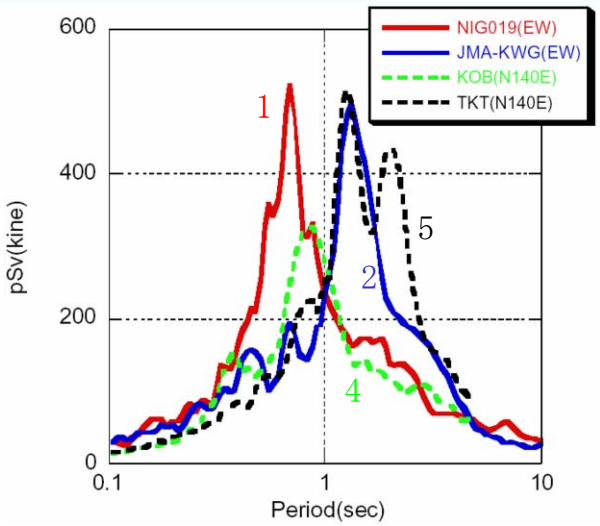

Fig. 2. Pseudo Velocity Response Spectra (AFRC IAIST, 2004).

This was the deadliest earthquake to strike Japan since January 1995's South-Hyogo earthquake (Kobe earthquake hereafter). The maximum acceleration of 1500 gal was recorded at Ojiya station, the nearest K-NET site to the hypocenter. This

acceleration was much greater than those recorded during the 1995 Kobe earthquake. Fig. 2 compares pseudo-velocity response spectra from both Chuetsu and Kobe earthquakes. Solid curves 1 and 2 show those from Chuetsu while broken curves 3 and 4 from the Kobe EQ of 1995. Curve 1, east-west component of K-NET Ojiya station (NIG019), is about identical to curve 4 from JMA Kobe observatory (KOB) for about all period components, but the response at K-NET Ojiya (curve 1) is larger than JMA Kobe (curve 3) for the periods ranging from 0.5 to 1.0 s. Curve 5, showing velocity response at Takatori (TKT), is also similar to that at JMA Kawaguchi observatory (curve 2) excluding that Takatori has its second peak at around 2 s.

2.2 *Damage to tunnels*

Kizawa Tunnel: The Kizawa tunnel skims the NW-SE trending branch of Futagoyama mountain ridge (Fig. 3). The area is covered with a thick Ushigakubi formation of Pliocene age. The surface configuration, shown in Fig. 3, indicates that Kizawa locality, about 300 to 800 m south of Mt. Futagoyama, lies on an old landslide mass with its escarpment, shown by line XX'. The south end of the tunnel is located a little below this escarpment. A depressed configuration is also found east to northeastern side along the Futagoyama ridge, suggesting the presence of another landslide escarpment (line YY'). The north end of the tunnel is closer to this configuration.

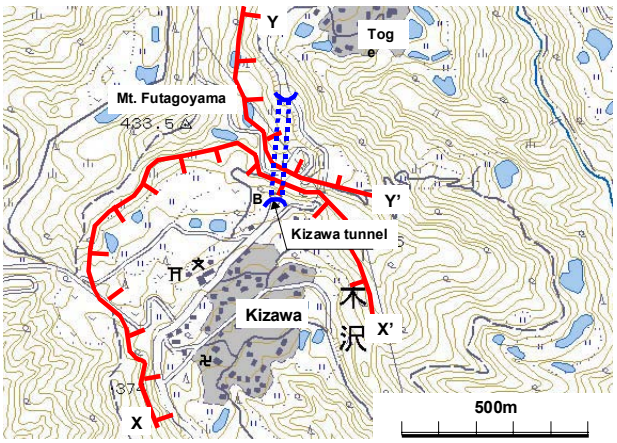

Fig. 3. Surface configuration in the vicinity of Kizawa tunnel.

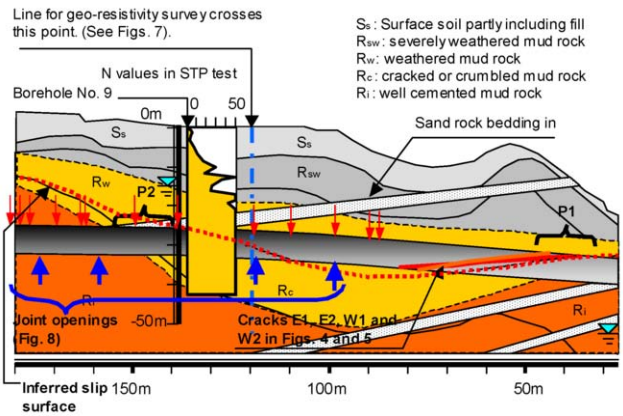

Fig. 4. Soil/rock profile along Kizawa tunnel: Downward thin arrows on the tunnel crown show locations of cracks cutting the tunnel axis upright and diagonally crosswise, while upward thick arrows show locations of joint openings (Konagai et al. 2005).

Fig. 4 shows the soil/rock profile along the tunnel. Though the rock layers forming this mountain exhibit a normally stratified geological structure sloping about 18 degrees towards SW (Yanagisawa et al. 1986), a different image of structure appears when the rocks are described in terms of their strengths. At two locations, P1 and P2, the northern part of the tunnel crosses a severely cracked and/or weakened mud rock layer overlying a depressed surface of an almost intact mud rock.

Northern 120 m segment of the Kizawa tunnel was laser-profiled. The image laser-profiled (Fig. 5) shows that two pairs of major cracks, E1, E2, and W1, W2, go diagonally up through the tunnel. The cracks, E1 and E2 on the east wall, extend over the 45 to 83m distance from the north tunnel end, while the cracks W1 and W2 extend over 38m to 88m distance on the west wall.

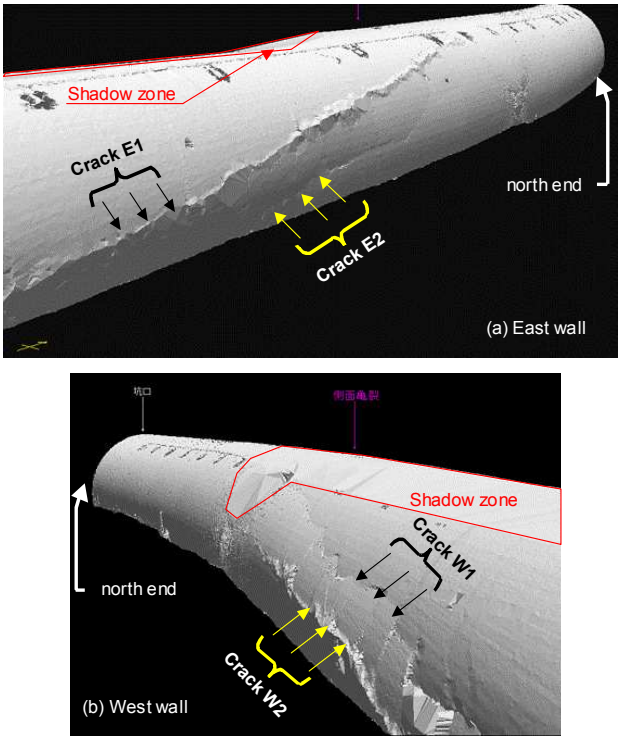

Fig. 5. Laser-profiled north segment of Kizawa tunnel (Konagai et al. 2005).

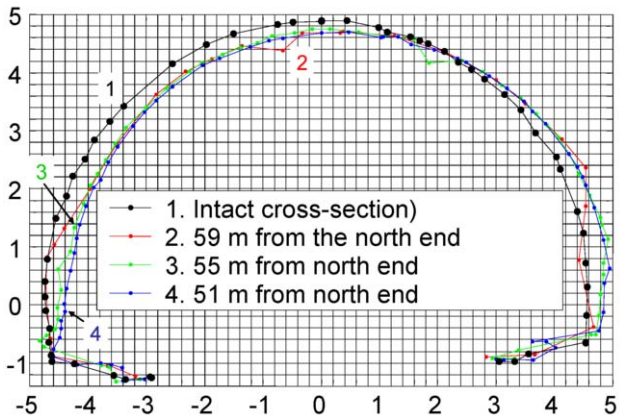

Fig. 6. Cross-sections of the cracked segment of Kizawa tunnel (Konagai et al. 2005).

Fig. 6 shows three tunnel cross-sections at 51, 55 and 59 m distances from the north end together with an intact cross section measured at the 100m distance. It is clear from this figure that the pairs of cracks on the wall became hinges for the upper half of the tunnel cross-section that was pushed 40 to 50 cm eastwards and about 10 cm down.

This part of the tunnel passes through a mountainside that slopes steeply down east, and the damage is considered to have

been caused by the movement of the soil/rock surrounding the tunnel, which was not clear in appearance from outside. As mentioned above, the northern part of the tunnel crosses at two locations, P1 and P2, a severely cracked and/or weakened mud rock layer (Fig. 5). The cracks E1, E2, W1 and W2 shown in Fig. 5 seem to be developed in this weakened mud rock zone P1 near the north tunnel end.

JR Shinkansen Uonuma Tunnel: The Uonuma tunnel, a 8,625 meter long concrete tunnel, crosses the inferred the Inokurayama fault (see Fig. 7), which is located just above the epicenter and the damage to the Uonuma tunnel may hint a reactivation of a small segment of this inferred fault. The Inokurayama fault stretches approximately 4 km in the SSE/NNW direction from its southern end, just east of Kawaguchi town, to the Konpira mountains in north with its west side as a hanging wall. of Uonuma tunnel (Konagai et al. 2005b).

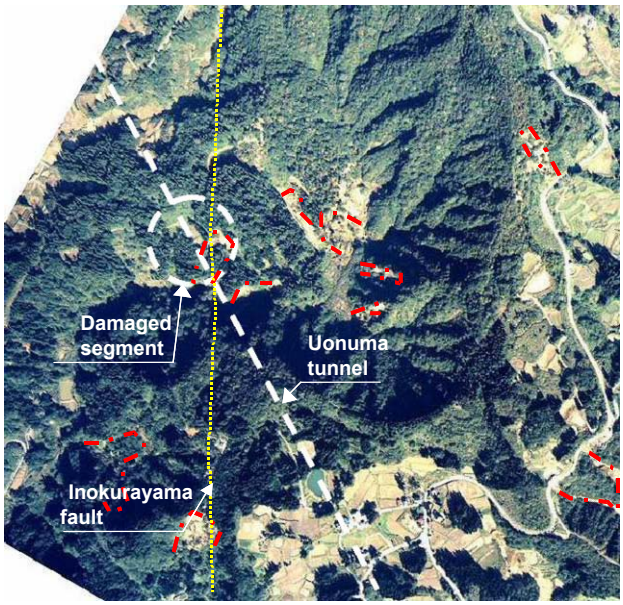

Fig. 7 Arial photograph of the area above the damaged segment

The tunnel was constructed through a squeezing rock zone, which spreads 120 m north ahead of the segment damaged in this earthquake. At the damaged location, the tunnel is about 60-100 meter deep. Cracks and their development of the damaged tunnel segment (Fig. 8a) over 195,060 to 195,080 m distance from Tokyo station are given in Figs. 8b and 8c. Several cracks cut the tunnel diagonally from the south to the center of the damaged area. These diagonal cracks merge at their southern ends to form a thrust dislocation showing about 13 cm shortening of the lining at this point. At the center of the damaged segment, the concrete crown broke up into large pieces, and fell in onto the rails and their slabs. The spalled part of the tunnel crown in Fig. 8c exposes steel supports. In Fig. 8c, the south part of the damaged area is to the right and the central part to the left. The northern part of the damaged segment (195,113m -) has lighter damage and the rail foundation was not deformed as much as in the south part (see Fig. 8a). However the center ditch along the rails shows a clear right-lateral shift of about 10-15 cm when it crosses this damaged part. NW-SE trending diagonal cracks were prevalent there.

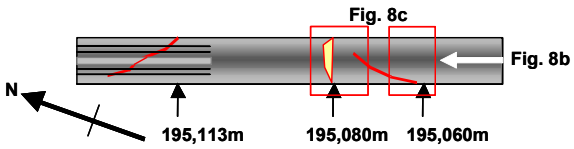

a) Damaged segment of Uonuma tunnel

b) Southern part of the damaged tunnel segment (from south to north)

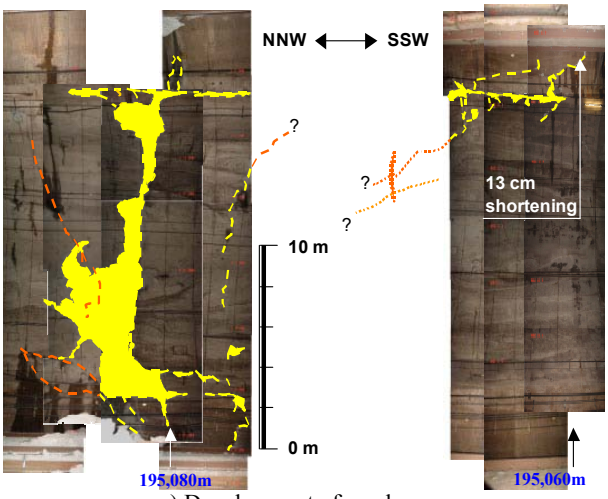

c) Development of cracks

Fig. 8. Cracks in the southern part of the damaged segment of Uonuma tunnel (195,060 - 195,080 m, Konagai et al. 2005b).

REFERENCES

Quick Report of the Oct. 23, Chuetsu Earthquake (2004): Active Fault research Center, National Institute of Advanced Industrial Science and Technology

Hirata, N. (2004): Quick report of aftershocks observation, Chuetsu earthquake of Oct. 23, 2004, http://www.eri.u-tokyo.ac.jp/hirata/chuetsu/041104yotiren4.pdf

Konagai, K., Numada, M., Zafeirakos, A., Johansson, J., Sadr, A. and Katagiri, T. (2005a): An example of landslide-inflicted damage to tunnel in the 2004 Mid-Niigata Prefecture earthquake, Landslides 2(2), 159-163, 2005.

Konagai, K., Zafeirakos, A., Numada, M., Johansson, J., Sadr, AA. and Katagiri, T. (2005b): Geotechnical hazard for civil-infrastructures in the October 23, 2004, Chuetsu earthquake, Bull., Earthquake Resistant Structure Research Center, IIS, University of Tokyo, 37.

3 SLOPE FAILURES BY KOKUSHO, T.

The damaged area is known as one of the landslide-prone areas of green tuff, with geological structures of active folding which cover active faults underneath. The synclines and anticlines are running parallel in the north-south direction, among which rivers are flowing in nearly the same direction. The mountains are about 400 m at the highest, and the slopes are composed of sedimentary soft rock of Neogene, which is alternative layers of strongly weathered mud stones and sand stones. Bedding planes have strong effects on the slope failure modes. More than 1,600 slope failures occurred due to the main shock and also several strong aftershocks. Some of the earthquake-induced slides were obviously influenced by previous landslides. Rainfall during three days immediately before the quake was 120 mm, which may have influenced the slope instabilities.

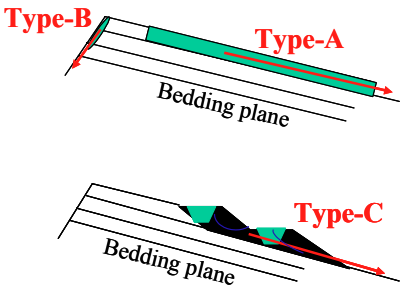

Fig. 1 Three types of slope failures; A, B and C, during the Niigataken Chuetsu earthquake.

The slope failures are classified into 3 types (Fig. 1):

Type-A: Deep slips parallel to sedimentation planes, in gentle slopes of around 20 degrees. In many cases, displaced soil mass had originally been destabilized by river erosions or road constructions, and behaved as a rigid body along the slip plane. The displaced soil volumes were very large, translating ground surfaces with little disturbance.

Type-B: Shallow slips of 1~2 m depth not parallel to sedimentation planes at steep slopes (> 30 degrees). This type far outnumbered Type-A, but the displaced soil volume was not so large. Soils normally fell down as pieces, sometimes leaving trees with deep roots at slopes.

Type-C: Deep slips in strongly weathered colluvial soils in places where ponds to cultivate carps (Koi-ponds) were located. This type seems very peculiar in this earthquake because countless Koi-ponds were located in the damaged area. This failure type obviously involved ponds, which seems to have provided water for piping and caused delayed flow-type failure of the debris. Soil liquefaction or cyclic softening may have contributed to large ground deformation including cracks because sand boils were actually witnessed at some sites.

Fig. 2. Landslide mass in Higashi-takezawa seen from the scarp.

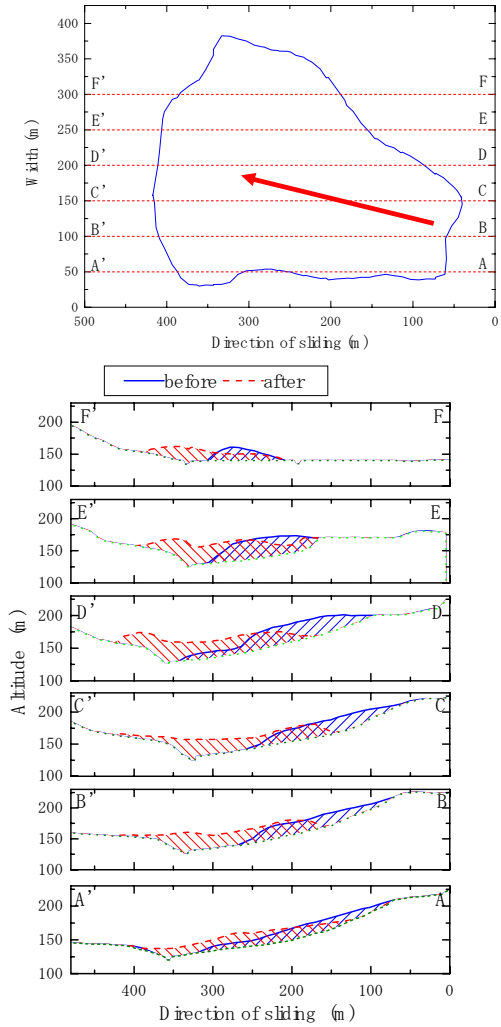

Fig. 3. Plan view (top) and cross- sectional views (bottom) of the slope failure shown in Fig. 2.

A number of slope failures stopped streams and made more than 80 natural reservoirs. The largest one inundated houses and eventually filled with sand sediments. Among different types of slope failures, Type-A made larger natural dams (soil volume of around 1.0 x10^6 m^3). Based on the energy approach (Kokusho et al. 2004), the shear strength exhibited along the slip surface was evaluated at Higashi Takezawa (one of the Type-A slope failures), of which the photograph is presented in Fig. 2. The cross-sectional change by the slope failure is illustrated in Fig. 3, from which the potential energy variation before and after the earthquake was calculated. The incident seismic wave energy at the site was evaluated based on nearby earthquake records at several sites around the site. The equivalent friction angle computed from the above two energies was 12.6° much lower than the angle of the slip plane 20°. This indicates that a drastic strength decrease occurred by some unknown mechanisms in highly weathered sandstone through which the slip plane is considered to have passed. Thus, it may be concluded that the sliding block was accelerated due to a small resistance and collided at the other side of the valley to plug the river flow and make the reservoir.

On the natural dams, emergency dewatering and spillway-constructions were implemented to prepare for flooding in next spring as shown in Fig. 4.

It was disclosed that similar disasters accompanying countless landslides in the green-tuff soft rock areas had occurred once in every 25 years on average in the north and central Main Island of Japan, the lessons of which had not been learned before.

Fig. 4 Spillway constructed on the natural dam in Higashi Takezawa.

REFERENCE

Kokusho, T., Ishizawa, T. and Harada, T. (2004): Energy approach for earthquake induced slope failure evaluation, Proc. 11th International Conference on Soil Dynamics & Earthquake Engineering and 3rd International Conference on Earthquake Geotechnical Engineering, Berkeley, California, Vol.2, 260-267.

4 DAMAGE TO EARTH STRUCTURES BY KOSEKI, J.

In this section, damage to earth structures for roads, railways and residential areas, as well as dams and river levees, are reported. The detailed information can be found in the relevant survey reports (e.g., JSCE, 2005 among others).

4.1 *Damage to Roads and Railways*

The conditions for damage to road embankments can be classified as follows.

a) Filled on valley.
b) Filled on uncemented debris or weathered terrace deposits.
c) Involved in large scale landslide.
d) With concentration of longitudinal or transverse ground water flow.
e) With liquefiable layer in the subsoil.

In terms with the number of damaged sites, many of them occurred under the conditions a) through c). Railway embankments were also damaged mainly under conditions a) and b). Typical example for each condition is herein shown briefly.

Fig. 1 shows an extensive slide of a road embankment constructed by filling a valley in a mountainous area along National Highway Route 290 (at Kuriyama-zawa, Tochio city). It should be noted that, as shown in the figure, a geogrid-reinforced embankment that had been constructed next to the collapsed unreinforced embankment was also damaged in the earthquake. This reinforced embankment had been constructed as a part of rehabilitation works for previous damage caused by rainfall.

Fig. 2 shows failure of a gravity type soil retaining wall along National Highway Route 17 at Tenno, Ojiya city. This wall had been constructed in parallel with a railway embankment, which also suffered from sliding failure as shown in the figure. These embankments had been filled on uncemented debris or weathered terrace deposits and were reconstructed by using geogrid-reinforced soil (GRS) retaining walls (Fig. 3). At the adjacent site, a railway embankment was reconstructed by using a combination of GRS retaining wall and ground anchoring.

Fig. 1. Collapsed road embankment along National Highway Route 290 at Kuriyama-zawa, Tochio city.

Fig. 2. Damage to embankments along National Highway Route 17 and JR Joetsu Line at Tenno, Ojiya city (by the courtesy of Ministry of Land, Infrastructure & Transport).

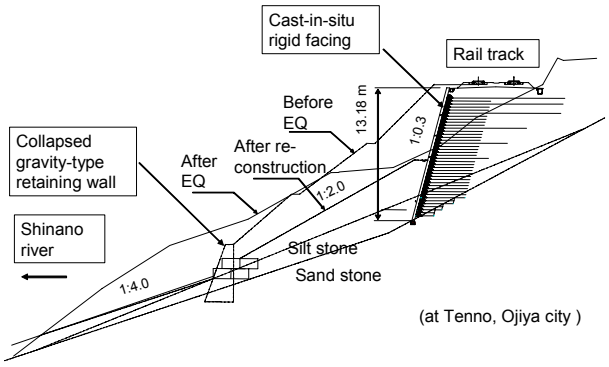

Fig. 3. Typical reconstruction of damaged railway embankment using geogrid-reinforced soil retaining wall (by the courtesy of JR-East).

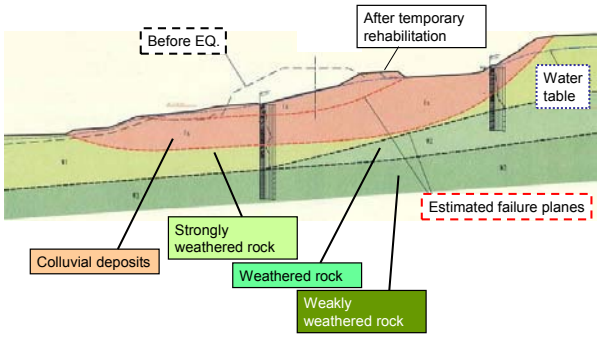

Fig. 4. Estimated soil profile of collapsed embankment along National Highway Route 290 at Kajigane, Yamakoshi Village (by the courtesy of MLIT).

Fig. 4 shows a cross-section of a collapsed embankment along National Highway Route 290 at Kajigane, Yamakoshi Village. This embankment was involved in earthquake-induced large scale landslide. In the reconstruction works for such a case, a careful judgment was required whether the landslide movement would restart again or not by possible heavy rainfalls in the future. It should be noted that, at the adjacent site, flow-type failure of embankment took place during the large aftershock, due possibly to water leakage from adjacent carp pond damaged by the mainshock.

Fig. 5 shows failure of an embankment along National Highway Route 8 at Miyamoto, Nagaoka city. It also shows a typical profile of SPT-N values. Road settlement and embankment deformation accumulated during several large aftershocks. During temporary rehabilitation works, it was confirmed that the ground water table was very high. Since there did not exist a liquefiable loose sandy soil layer in the subsoil, concentration of longitudinal or transverse ground water flow into soft clayey subsoil layers that was magnified by the preceding heavy rainfall was considered to be the major cause for the failure. During the reconstruction works, the subsoil layers were improved by installing gravel compaction piles.

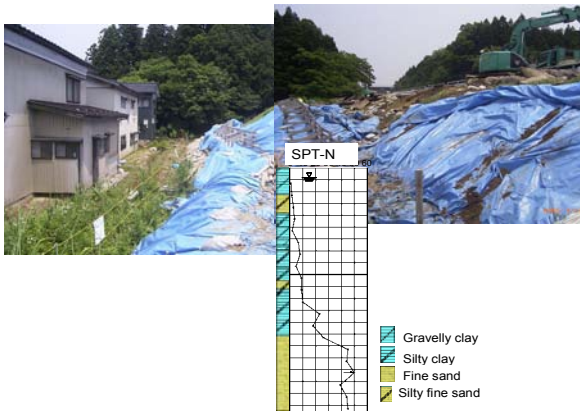

Fig. 5 Failure of road embankment along National Highway Route 8 at Miyamoto, Nagaoka city and typical profile of SPT-N values (by the courtesy of MLIT).

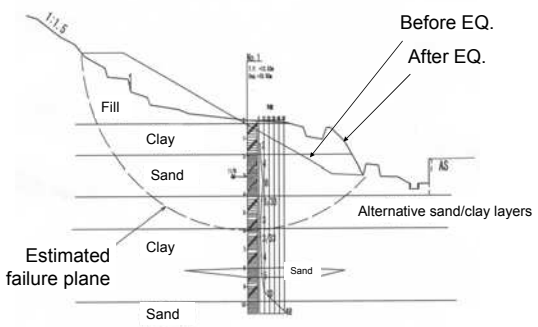

Fig. 6. Estimated soil profile of failed abutment embankment at Mitsuke-Ohashi bridge, National Highway Route 8 (by the courtesy of MLIT).

Fig. 6 shows a cross section of a failed abutment embankment at Mitsuke-Ohashi bridge, National Highway Route 8. In this case, a loose sandy layer existed below the ground water table, which is estimated to have liquefied during the earthquake. During the reconstruction works, the subsoil layers were improved by installing in-situ cement-mixed piles by jet grouting method.

Fig. 7. Collapsed embankment for regional road around a newly-developed building estate at Taka-machi, Nagaoka city.

4.2 *Damage in Residential Areas*

Several newly-developed building estates were affected by the damage to earth structures.

Figure 7 shows collapse of an embankment for regional road around a newly-developed building estate at Taka-machi, Nagaoka city. The estates were constructed by cutting hills and filling valleys. The filled portions along their outer rim were severely damaged due possibly to insufficient compaction and drainage capacity of the fill materials, causing uneven settlement of the adjacent building foundations. They were reconstructed by using GRS retaining walls.

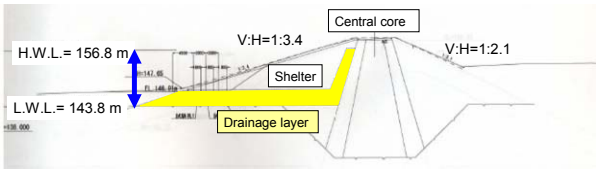

Fig. 8. Typical cross section of Shin Yamamoto Dam (by the courtesy of JR-East).

4.3 *Damage to Dams*

Three rockfill dams consisting of Shinano River Power Plants operated by JR East Company were damaged by the earthquake. Among them, damage to Shin Yamamoto Dam that was completed the most recently in 1990 will be reported herein.

As shown in Fig. 8, Shin Yamamoto Dam is a 42.4 m-high central core type, which is sandwiched by shelter zones with an upstream drainage layer. The shelter materials had been taken from nearby river terrace deposits, which consisted of round particles with a maximum diameter of about 400 mm. By the earthquake, the dam suffered crest settlements that were rather proportional to the dam height at each survey point. Their maximum value was about 0.8 m. As influential factors, following issues are being investigated by the survey committee:

a) cyclic compaction in relatively local loose sub-layers in the shelter zone,
b) directionality of earthquake motions,
c) several large aftershocks,
d) possible washout of fine contents from the upper shelter zone caused by the daily change in the water level and associated clogging of the drainage layer, and
e) thick sedimentation of fines content included in the river water in the reservoir and associated closing the outlet of the drainage layer.

4.4 *Damage to River Levees*

Damage to river levees were caused mainly by liquefaction of subsoil layers. Most of the damage was accompanied by sand boils in the subsoil layers at the foot of the levees.

Fig. 9. Damage to levees along Shinano river; a) crest settlement at Namiki-shinden, Nakanoshima-machi (by courtesy of Mr. Ishihara,M., PWRI); and b) failure of concrete revetment at Chiya, Ojiya city (by the courtesy of MLIT).

Large scale damage such as the one shown in Fig. 9a occurred in moderately-shaken regions where liquefiable layers existed in the subsoil. In severely-shaken regions, on the other hand, the extent of the damage was rather limited as typically shown in Fig. 9b, since these regions were located on the upstream side of the river, where liquefiable layers in the subsoil existed only locally.

4.5 *Summary*

In summary, different failure patterns and causes were observed/estimated in the case histories on damage to earth structures during the 2004 Niigata-ken Chuetsu earthquake. Several influential factors can be pointed out, such as a) heavy rainfalls preceding the earthquake, b) large aftershocks, c) geological conditions for subsoil including existence of liquefiable layers, d) compaction degrees for embankment, and e) drainage capacity from subsoil/embankments. In the reconstruction works of damaged roads and railways, preferred use of geogrid-reinforced soil retaining walls was implemented.

REFERENCE

JSCE (2005): Damage survey report of the 2004 Niigata-ken Chuetsu earthquake (in print) (in Japanese).

5 LIQUEFACTION AND LIFELINE DAMAGE BY MIYAJIMA, M.

In this section, liquefaction and lifeline damage, especially liquefaction-induced lifeline damage, are reported.

5.1 *Soil Liquefaction*

Fig. 1 shows soil liquefaction sites that were found by field investigation and aerial photographs (Wakamatsu et al. 2005), Photo. 1 shows a typical aerial photograph taken immediately after the earthquake. Light portions seen in the paddy fields in the photograph indicate sand volcanoes caused by soil liquefaction in the ground. According to Fig. 1, soil liquefaction mostly occurred along the riverside of Shinano River and its branches between Yoita Town and Tokamachi City. A distance from the epicenter of the main shock to the liquefied sites was within 30 km.

Soil liquefaction occurred in Mitsuke City is explained herein as a typical case. Photo. 2a shows soil liquefaction sites on an aerial photograph of Mitsuke City. Black dots indicate sand volcanoes caused by soil liquefaction. Balck dots shown in Photo. 2b indicate wooden houses damaged at roofing tiles. Photo. 3a indicates an aerial photograph of Mitsuke City in 1984. Kariyata River was winding and back dots indicating soil liquefaction spots coincide with the old river bed at that time. On the other hand, black dots in Phote. 3b indicate damage to

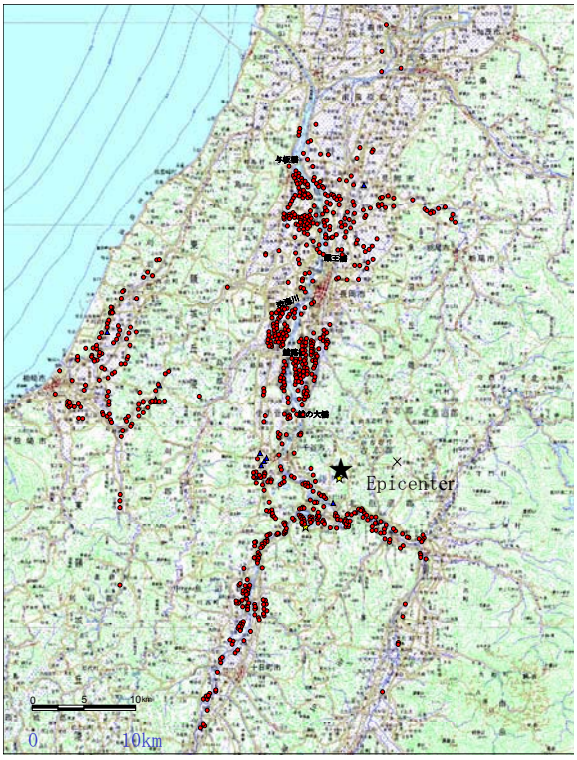

Fig. 1. Soil liquefaction sites (dark dot) found by field investigation and aerial photograph in the 2004 Niigata-ken Chuetsu Earthquake (Wakamatsu et al. 2005).

Photo. 1. Aerial photograph of Yoita Town taken immediately after the earthquake (taken 24 Oct. 2004, by the courtesy of Asahi Kogyo Co. Ltd.).

roofing tiles. The area of these black dots in Photo. 3b does not coincide with that of the black dots in Photo. 3a: that is, damage to roofing tiles did not occurred at the liquefied sites. This fact seems to be related to a difference in the predominant frequency between the liquefied ground and these wooden houses with roofing tiles.

Soil liquefaction has also occurred in this region in the 1964 Niigata Earthquake. Soil liquefaction occurred again at nearly the same sites in the 2004 earthquake.

5.2 *Liquefaction-Induced Lifeline Damage*

Damage induced by soil liquefaction such as cracks in the pavement of road and its subsidence, subsidence of houses, pull-out at joint of water supply pipelines, uplift of sewerage manhole etc., was not sever

a)

b)

Photo. 2 a) Sand volcanoes (white dots); and b) wooded houses damaged at roofing tiles (white dots) on an aerial photograph in these days (Bando et al. 2005).

a)

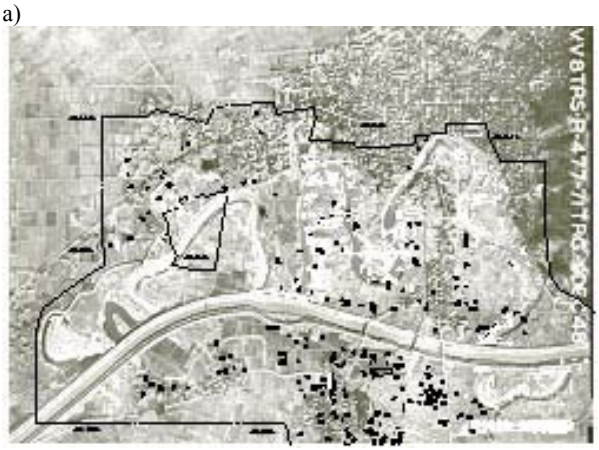

b)

Photo. 3 a) Sand volcanoes (white dots;) and b) wooded houses damaged at roofing tiles (white dots) on an aerial photograph in 1948 (Bando et al. 2005).

Photo. 4 shows a typical case of the subsidence of a wooden house that occurred at Mitsuke City. Cracks of the ground of the foundation appeared and subsidence of surface ground and foundation of house was caused by soil liquefaction.

Photo. 5 indicates damage to a water supply pipeline in Ojiya City. Pull-out at joint of ductile iron pipe occurred at soil liquefaction sites. Since sand ejection happened from the backfill sand, the liquefaction of the backfill seems to be one of the causes of damage. The total number of failures for service and distribution pipelines was 102 in Ojiya City. The damage ratio, defined as the amount of failure per length of pipeline, was 0.31/km in Ojiya City. In Nagaoka City, 287 failures for service and distribution pipelines occurred and the damage ratio was 0.26/km. Liquefaction-induced damage to water supply pipeline was, however, relatively light.

Photo. 6 shows an uplift of a sewerage manhole in Nagaoka City. This is typical of over a thousand occurrences of distributed manholes that were observed throughout the region. Buried sewerage lines were also disrupted due to permanent ground deformation. The total length of damaged pipelines was 152.1 km and the total number of damaged manholes was 2,719. Similar phenomena appeared during the earthquake occurred in Hokkaido, for example, the 1993 Kushiro-oki Earthquake, the 1994 Hokkaido Toho-oki Earthquake, 2003 Tokachi-oki Earthquake and so on, as shown in Photo. 7.

Fig. 2 is a schematic diagram of a section of sewerage manhole that is damaged by the liquefaction in the backfill (Yasuda et al. 2004). The surrounding soil of sewerage line was peat in Hokkaido and very soft silt or clay in Niigata. These materials have a low permeability and are very soft. Moreover the backfill sand of sewerage line was relatively loose and the underground water level was high during the earthquake. The backfill sand was, therefore, very liquefiable because the backfill sand easily deformed under undrained conditions during the earthquake.

REFERENCES

Bando, K., Saito, H., Urayama, T. and Abeki, N. (2005): Relation between building damage and the ground in Mitsuke urban area due to the mid Niigata prefecture earthquake in 2004, Proceedings of the 40th Japan National Conference of Geotechnical Engineering, pp. 2121-2122.

Wakamatsu, K., Yoshida, N. and Kiku, H. (2005): Liquefaction during the 2004 Niigata-ken Chuetsu earthquake, Proceedings of the 40th Japan National Conference of Geotechnical Engineering, 2215-2216

Yasuda, S. et al. (2004): Report of geo-hazards in the 2003 Tokachi-oki earthquake, Japanese Geotechnical Society, 111-120.

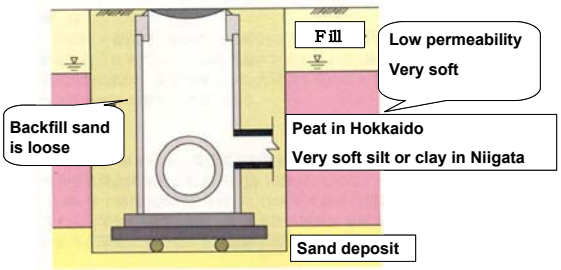

Fig. 2. Schematic diagram of a section of sewerage manhole (Yasuda et al., 2004).

Photo 4. Subsidence of a wooden house induced by soil liquefaction, Mitauke City.

Photo 5. Pull-out at joint of water supply pipelines, Ojiya City.

Photo 6. Uplift of sewerage manhole, Nagaoka City.

Photo 7. Uplift of sewerage manholes at Toyokoro Town (2003) and Shibetsu Town (1994), Hokkaido.